École Nationale Supérieure de l'Énergie, l'Eau et l'Environnement

Research Project

Adaptive Speed Control of an Autonomous Vehicle with a Comfort Objective

Students:

Eduarda Karoliny COSTA **(IEE)**

Gia Quoc Bao TRAN **(ASI)**

Supervisor:

Professor. Olivier SENAME

(GIPSA-lab)

Contents

1 Introduction

In a first step, a bibliographical research was done. We read some articles and books, as given in the chapter 6 - References. In particular the most relevant Y. Du, C. Liu and Y. Li, "Velocity Control Strategies to Improve Automated Vehicle Driving Comfort" (1) and "Robust Control Design for Active Driver Assistance Systems. A Linear-Parameter-Varying Approach"(4).

Our goal from the start was to define the speed of the autonomous car with a view to comfort and then track it using a suitable controller that guarantees robustness. The research was divided into two parts: find a reference speed in view of the comfort (by Eduarda) and control the autonomous car (by Bao). Then the two main parts were combined into what we call the comfort-oriented speed control strategy. Finally, we performed an evaluation of driving comfort and demonstrated the trade-off between this and high speed.

The diagram below represents the complete scope of the project.

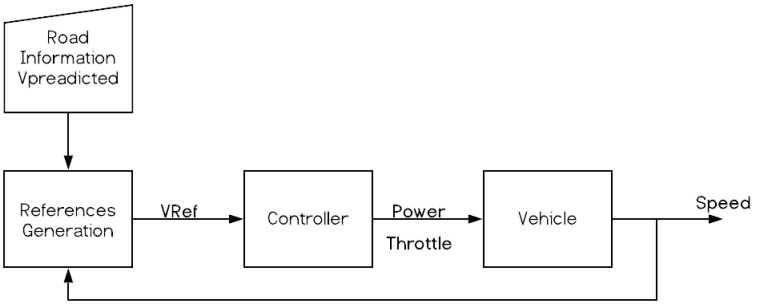

Figure 1: The diagram that represents the project

2 How to select a reference speed accounting for comfort objectives (This part has been mainly handled by Eduarda)

2.1 The Quarter Car Model (QCM)

Driving comfort can be evaluated by the multiple accelerators fixed inside vehicles. In order to quantify comfort, we need to analyse the effect of road vibration on the car body. For this purpose, a model was used for the representation of the vehicle, called the "Quarter Car Model" (QCM). The QCM is a vehicle model that can effectively be used to study the dynamic interaction between vehicle and road roughness profile, and therefore in the study of vibrations generated by the road. By combining the masses values m, the stiffness constant k and damping c of the QCM, it is possible to model any type of road vehicle: car, bus or truck. (2)

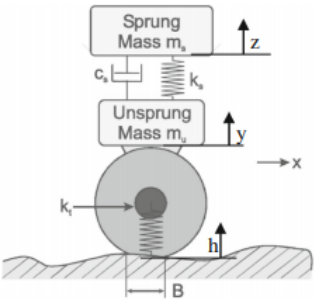

Figure 2: QCM - quarter car model

2.2 The road profile

For the research project, we used a function that was developed by GIPSA-lab members. This MATLAB® function implements the QCM model together with the classification of the road profiles according to ISO8606. We used two types of car models as parameters for the tests: a real Megane car with data provided by previous research done by the GIPSA-lab laboratory. And a small 1/5 scaled car, the Inove, positioned on the laboratory's test platform. We can notice the big difference between them, by the maximum speed they can reach. The Megane reaches 140 Km/h and the Inove 45 Km/h. Our objective is to simulate the effect of carious road profiles, at different speeds, and to evaluate the comfort. The equation to calculate the different road profiles based on QCM and the ISO8606 standard:

$$\dot{Z}_r(s) + \Omega_c Z_r(s) = 2\pi\eta_o\sqrt{S_q(\eta_o)}W(s) \tag{1}$$

ω_c is the road spatial cut-off angular frequency $\omega_c = 2\pi\eta_o$

η_c is the road spatial cut-off frequency $\eta_o = 0.01(m^{-1})$

η_0 is the standard spatial frequency $\eta_c = 0.1(m^{-1})$

$W(s)$ is the white noise in the space-domain

According to the space-time relationship, we have: $\dot{s}\frac{\mathrm{d}}{\mathrm{d}s} = \frac{\mathrm{d}}{\mathrm{d}t}$

Substituting equation according to the space-time into the equation (1), the road excitation in non-stationary running process can be rewritten as:

$$\dot{Z}_r(t) + \dot{s}\Omega_c Z_r(t) = 2\pi\eta_o\sqrt{G_d(\eta_o)}W(t) \tag{2}$$

Where $\dot{s}$ is given as $\dot{s} = v_o + at$ in which, v_o is the initial vehicle velocity and a is the acceleration of the vehicle;

t is the time running period of the vehicle and $S_q(\eta_o) = \sqrt{G_d(\eta_o)}$. We consider $a_1 = 2\pi\eta_c$, $b_1 = 2\pi\eta_o\sqrt{G_d(\eta_o)}$, so the equation will become:

$$\dot{Z}_r(t) + Va_1Z_r(t) = b_1VW(t) \tag{3}$$

Bases on the *ISO 8608:2016*, the road is divided into several types A, B, C, D, E, H as in the table below:

Road class	Degree of roughness			
	Lower limit	Geometric mean	Upper limit	Geometric mean
	Spatial frequency units, n			
	$G_d(n_0)^a$ 10^{-6} m^3			$G_v(n)$ 10^{-6} m
A	—	16	32	6,3
B	32	64	128	25,3
C	128	256	512	101,1
D	512	1 024	2 048	404,3
E	2 048	4 094	8 192	1 617
F	8 192	16 384	32 768	6 468
G	32 768	65 536	131 072	25 873
H	131 072	262 144	—	103 490

Figure 3: The degree of road roughness

Due to the large unstability and variation perceived from class E, it was decided to analyze and perform the tests only up to class D. We can see in the images that the road profiles are well adapted to the dimensions of each car.

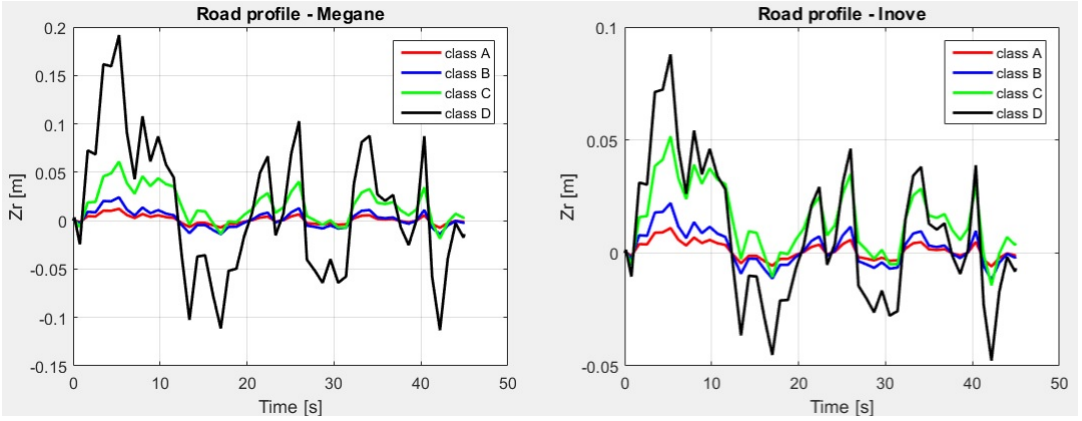

Figure 4: Road profile Megane et Inove

2.3 The classification of road profiles according to the comfort

The use of ISO 2631 is based on the assumption that a given road has equal statistical properties everywhere along a section to be classified. That is: the road surface is a combination of a large number of longer and shorter periodic bumps with different amplitudes. The combination is the same wherever one looks along the road section.

After drawing the eight road profiles described in the ISO 2631, we use a weight to filter the sprung mass acceleration in order to evaluate the passenger comfort in the human frequency range. The filter's transfer

function is described below:

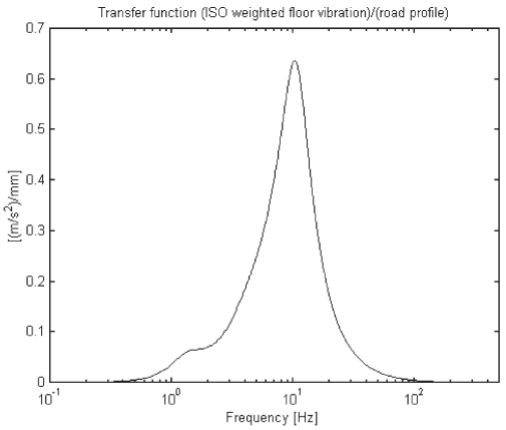

FIGURE 4 Transfer function (ISO W_k weighted floor vibration)/(road roughness profile elevation).

Figure 5: Filter response in frequence mode

$$W_{iso} = \frac{81.89S^3 + 796.6S^2 + 1937S + 0.1446}{S^4 + 80S^3 + 2264S^2 + 7172S + 21196} \tag{4}$$

We can see in the images that the road profiles are well adapted to the dimensions of each car.

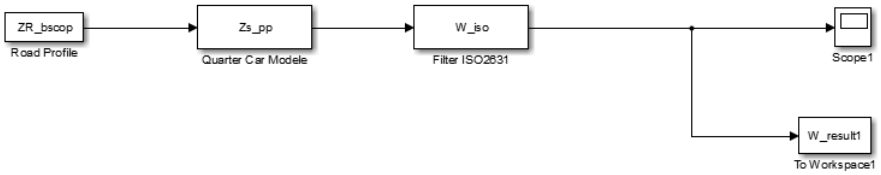

Figure 6: The Schematic with ISO 2631

It is possible to see in the figure below the difference between the two car parameters, as well as the result in the Road Profile values before and after the filter. A speed of $80km/h$ was used for the model below.

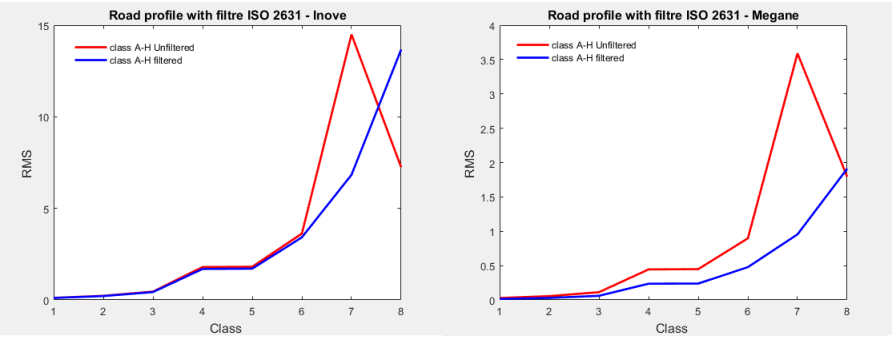

Figure 7: Graph Road Profile with filter ISO 2631

2.4 The International Roughness Index (IRI)

The International Roughness Index (IRI) was developed by the World Bank in the 1980s for uniform evaluation of infrastructure in developing countries, which is described by Gillesepie et al(5). The IRI is a scale (m/km) for roughness based on the response of a generic motor vehicle (referred as Golden Car) to roughness of thread surface. The values are calculated using a quarter car vehicle model, whose response at a speed of 80 km/h is accumulated to yield a roughness index with units of slopes. To obtain the IRI values, the following formula was implemented in MATLAB®:

$$IRI = \frac{1}{L}\int_0^{\frac{L}{V}} \left|\dot{Z}_s - \dot{Z}_u\right| dt \tag{5}$$

In this equation we have for L a value of 1 Km and for V a value of 80 Km/h. When we plotted the graphs between, the IRI values and the RMS (root mean square) of suspension displacement we have for each point on the graph, a IRI values of different road types are compared with physically measured RMS suspension displacement values. It is possible to see, for the two models of car, that there is a linear relationship between the two magnitudes (IRI and RMS suspension displacement).

For RMS values it is possible calculate with:

$$a_{wz} = \sqrt{\sum_{i=1}^{23}(W_{k,i}a_{iz})^2} \tag{6}$$

Where $W_{k,i}$ are the frequency weightings in one-third octaves bands for the seated position, provided by the standards and a_{iz} is the vertical RMS.

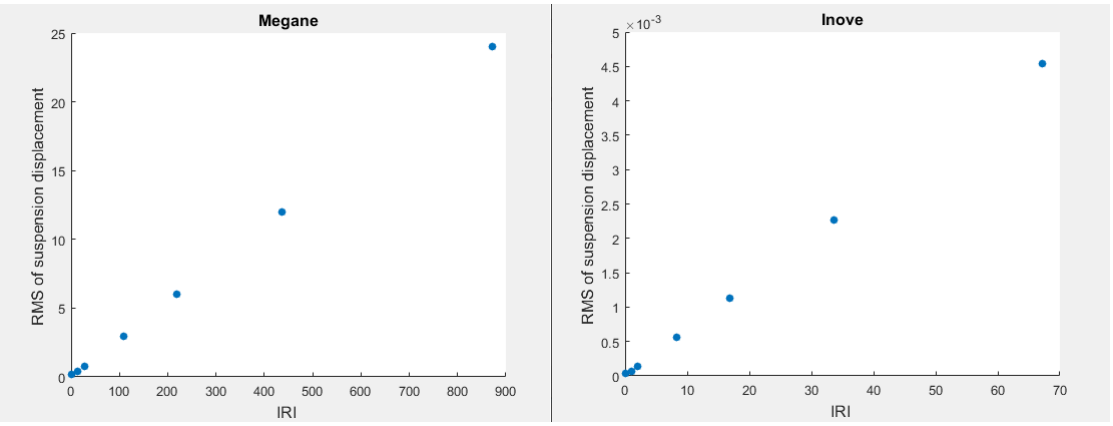

Figure 8: RMS of suspension displacement x IRI

After applying the filter, we decided to analyze the influence of speed variation on our results. For each road profile was changed at a speed of 30 Km/h to 100 Km/h with a variation of 10 Km/h and was related to each

RMS value.

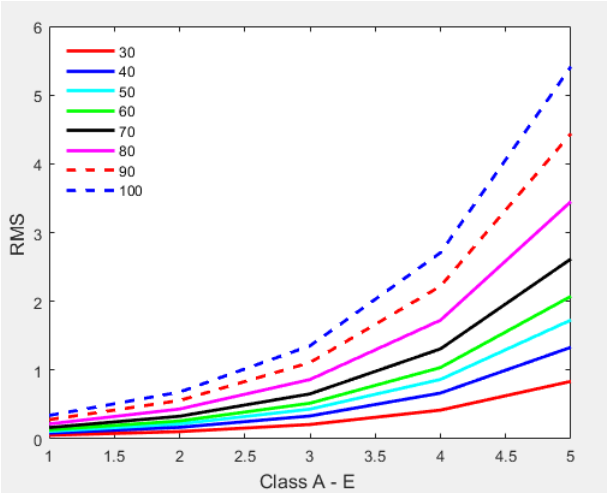

Figure 9: RMS values with different speeds for road profile

In ISO2631 we find a table that allows us to evaluate the comfort according to the calculated RMS value. We use this table to draw scenarios in order to control the speed with a view to comfort.

Scale of discomfort suggested in BS 6841 [1] and ISO 2631 [2]

Less than 0·315 m/s^2	Not uncomfortable
0·315–0·63 m/s^2	A little uncomfortable
0·5–1 m/s^2	Fairly uncomfortable
0·8–1·6 m/s^2	Uncomfortable
1·25–2·5 m/s^2	Very uncomfortable
Greater than 2 m/s^2	Extremely uncomfortable

Figure 10: Scale of discomfort

In the graph we consider the number 1 to class A following in order until class D when analyzing the graph taking into consideration the *ISO2631* table. It is possible to notice that as we have a road profile with higher vibrations, the higher is our RMS, and the lower is the permitted variation for speed, if we want to respect an exact level of comfort.

2.5 Relationship between speed and RMS value

To find a reference speed, we have decided to draw the RMS values for each road profile according to the table below:

RMS values (awz for each class)					
Velocité	Classe A	Classe B	Classe C	Classe D	Classe E
30	0.0525	0.1051	0.209	0.418	0.8361
40	0.0837	0.1673	0.3329	0.6658	1.3315
50	0.1086	0.2171	0.432	0.864	1.7280
60	0.1303	0.2605	0.5183	1.0367	2.0734
70	0.1644	0.3288	0.6542	1.3083	2.6166
80	0.2168	0.4336	0.8627	1.7254	3.4507
90	0.2789	0.5577	1.1097	2.2194	4.4388
100	0.3401	0.6801	1.3532	2.7065	5.4129
110	0.4008	0.8015	1.5948	3.1896	6.3792
120	0.4610	0.9220	1.8344	3.6689	7.3378
130	0.5187	1.0373	2.0639	4.1279	8.2558

Scenarios			
Road Profile Class	RMS	Comfort Level	Speed variation (Km/h)
A,B,C,D	0.315 - 0.63	A little Uncomfortable	30
A,B,C	0.315 - 0.63	A little Uncomfortable	30 - 60
A, B	0.315 - 0.63	A little Uncomfortable	30 - 90
A,B,C,D,E	0,5 - 1	Fairly Uncomfortable	30
A,B,C,D	0,5 - 1	Fairly Uncomfortable	30 - 50
A,B,C	0,5 - 1	Fairly Uncomfortable	30 - 80
A,B	0,5 - 1	Fairly Uncomfortable	30 - 120
A,B,C,D,E	0.8 - 1,6	Uncomfortable	30 -40
A,B,C,D	0.8 - 1,6	Uncomfortable	30 - 70
A,B,C	0.8 - 1,6	Uncomfortable	30 - 110
A,B	0.8 - 1,6	Uncomfortable	30 - 120

Figure 11: RMS values and scenarios

From this data we used MATLAB's Polyfit function, so it was possible to obtain a polynomial that calculates the RMS value according to the speed for each road profile. The graphic below shows the curve between speed and RMS values, and the points are the polynomial values at each speed.

As the values above 100 km/h resulted in very large values of RMS, it was decided to take them out of analysis. Values in m/s were used to build the polynomial below.

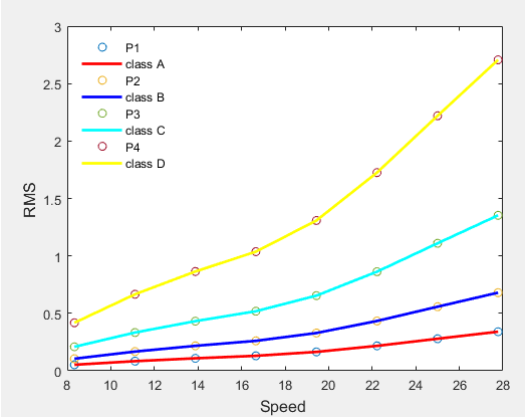

Figure 12: Polynomial RMS (speed)

For Class A we have:

$$RMS = -0.0065V^3 + 0.0772V^2 - 0.4558V + 1.0822 \tag{7}$$

For Class B we have:

$$RMS = -0.0138V^3 + 0.1633V^2 - 0.9599V + 2.2735 \tag{8}$$

For Class C we have:

$$RMS = -0.0283V^3 + 0.3323V^2 - 1.9480V + 4.6047 \tag{9}$$

For Class D we have:

$$RMS = -0.0531V^3 + 0.6303V^2 - 3.7162V + 8.8175 \tag{10}$$

3 Longitudinal control of the vehicle (This part has been mainly handled by Bao)

3.1 Car longitudinal dynamics and system's state-space representation

Suppose we have a car of mass m travelling at the speed of v. Let F be the control force on the car (from the road, also equals the control force exerted by the engine), and F_d the total disturbance force. We have the following equation of motion:

$$m\dot{v} = F - F_d \tag{11}$$

The disturbance force comprises three components: the rolling friction supposed to have a constant value, the drag by gravity supposing the road's slope θ to be sufficiently small (between $\pm 10°$), and the aerodynamic drag adding non-linearity to the system:

$$F_r = mgC_r \tag{12}$$

$$F_g = mg(\theta) \tag{13}$$

$$F_a = \frac{1}{2} C_v \rho S v^2 \tag{14}$$

In which C_r is the rolling friction coefficient, is ρ the air's density, S represents the car's frontal area, and C_v is the aerodynamic drag coefficient. The disturbance force thus has the following equation:

$$F_d = mgC_r + mg(\theta) + \frac{1}{2} C_v \rho S v^2 \tag{15}$$

Finally, the car's motion equation is formulated as:

$$m\dot{v} = F - mgC_r - mg(\theta) - \frac{1}{2} C_v \rho S v^2 \tag{16}$$

The forces acting on the car are demonstrated in the following figure:

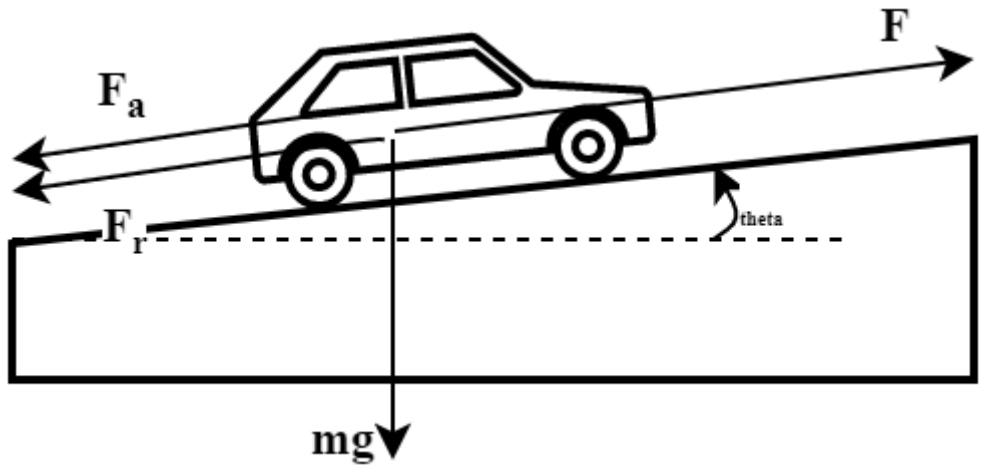

Figure 13: Forces acting on the vehicle

For our simulations, the values are as follows:

Symbol	Value	SI unit	Parameter name
m	1410	kg	Car's mass
C_r	0.01	-	Rolling resistance coefficient
C_v	0.32	-	Aerodynamic resistance coefficient
ρ	1.3	kg/m^3	Density of air
S	2.4	m^2	Car's frontal area
g	9.8	m/s^2	Gravitational acceleration
F_{max}	4000	N	The engine's maximum force

Before we can study the longitudinal dynamics, we need to define its state-space representation. The only state variable here is the car's speed which is also the measured output, with the control input being the force F:

$$\dot{v} = \frac{1}{m}(F - mgC_r - mg(\theta) - \frac{1}{2}C_v\rho S v^2) = f(v,u) \tag{17}$$

$$y = v = g(v,u) \tag{18}$$

To study the system, we need to linearize it around an equilibrium point defined by the set (v_0, u_0, θ_0) as:

$$0 = u_0 - mgC_r - \frac{1}{2}C_v\rho S v_0^2 - mg\theta_0 \tag{19}$$

For our simulations, the initial car speed is 20 m/s and the initial slope depends on which slope profile we want

to test the system (there are a random slope profile and another one given from a study of Balázs Németh (8)), and the initial control signal is therefore determined accordingly. We obtain the following linear state-space representation:

$$\dot{\tilde{v}} = A\tilde{v} + B\tilde{u} \tag{20}$$

$$y = C\tilde{v} + D\tilde{u} \tag{21}$$

$$A = -\frac{\rho S C_v v_0}{m} \tag{22}$$

$$B = \frac{1}{m} \tag{23}$$

$$C = 1 \tag{24}$$

$$D = 0 \tag{25}$$

The matrix A is of order 1 and has a negative eigenvalue which means the open-loop system is stable. We have only one state variable and looking at the matrices B and C, we see that it is both controllable and observable. So we can find a linear controller and do not need an observer.

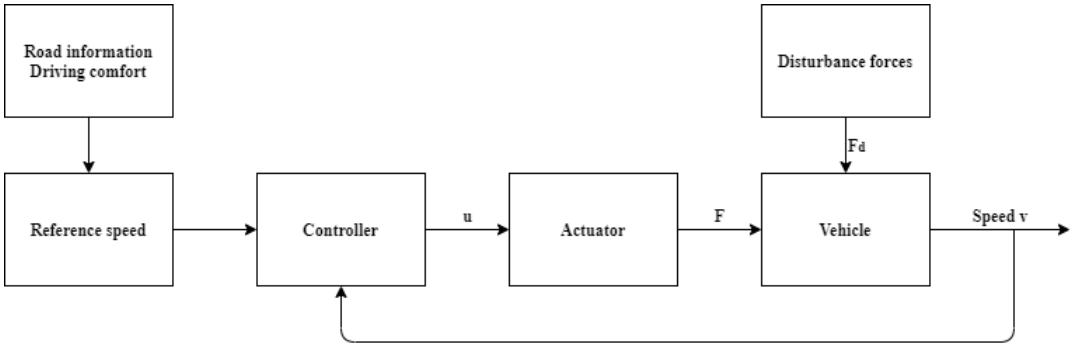

Figure 14: Block diagram of the closed-loop longitudinal control system

The objective of the control part is to track a reference speed while being insensitive to the disturbance inputs coming from the slope variations and the wind.

3.2 Longitudinal control approaches

3.2.1 Objectives and necessary assumptions

The objectives of this core part are to:

- Establish effectively controllers that would guarantee the following requirements: the car needs to be able to track certain reference speed profiles, and it must do so in the presence of disturbances and uncertainties.

- Test the controllers under those mentioned circumstances.

- Analyze the controllers in terms of robustness, or the ability to perform sufficiently well in cases where the parameters used for their design and those in reality are different.

- Conclude the best controller which satisfies the tests the most successfully.

To do the above, we have these prior assumptions:

- The car's mass is measured on-line using multiple built-in sensors that detect the additional load. This is the most crucial assumption as it allows for gain-scheduling based on mass and the performance of the system relies heavily on this particular parameter.

- The road slope can be known/estimated in real-time thanks to the car being a connected vehicle. This is the condition that enables the making of a compensation strategy, which counters the slope disturbance.

3.2.2 Static linear quadratic regulator (LQR) with integral action

The control signal consists of:

$$u(t) = u_0 + \tilde{u}(t) = u_0 + \tilde{u}_{feedback}(t) \tag{26}$$

The offset can be omitted due to the system's low non-linearity. To reject the effect of the disturbance forces, we can use a state-feedback controller with integral action. Let z be the integral of the error, v_0 be the reference linearized speed, that is the difference between the real reference speed and the equilibrium one:

$$\dot{z}(t) = v_0(t) - \tilde{v}(t) \tag{27}$$

We extend the state-space representation:

$$\begin{bmatrix} \dot{\tilde{v}} \\ \dot{z} \end{bmatrix} = \begin{bmatrix} A & 0 \\ -C & 0 \end{bmatrix} \begin{bmatrix} \tilde{v} \\ z \end{bmatrix} + \begin{bmatrix} B \\ 0 \end{bmatrix} \tilde{u} + \begin{bmatrix} 0 \\ 1 \end{bmatrix} r + \begin{bmatrix} E \\ 0 \end{bmatrix} d \tag{28}$$

$$y = \begin{bmatrix} C & 0 \end{bmatrix} \begin{bmatrix} \tilde{v} \\ z \end{bmatrix} \tag{29}$$

In which d represents the (small) disturbances and E is its corresponding vector. It has been known that integral action will enable disturbance rejection (we do not re-prove that here).

Our static state-feedback controller with integral action has the form:

$$\tilde{u}_{feedback}(t) = -\begin{bmatrix} F & H \end{bmatrix} \begin{bmatrix} \tilde{v} \\ z \end{bmatrix} \tag{30}$$

And then the gains F and H would be calculated so as to minimize the linear quadratic criterion:

$$J = \int_0^\infty (x^T(t)Qx(t) + u^T(t)Ru(t))dt \tag{31}$$

In which x is the extended state vector:

$$x = \begin{bmatrix} \tilde{v} \\ z \end{bmatrix} \tag{32}$$

In order to lay emphasis on the rejection of disturbances, equal weights were given to the states, and the control signal's weight were tuned so as to keep it at the point of not saturating most of the time. Results would be presented in the validation parts.

3.2.3 Gain-scheduled LQR with integral action

The control signal's feedback part is an LQR with integral action:

$$\tilde{u}_{feedback}(t) = -\begin{bmatrix} F(m,v) & H(m,v) \end{bmatrix} \begin{bmatrix} \tilde{v} \\ z \end{bmatrix} \tag{33}$$

Of which the gains are scheduled according to a grid-based linear parameter-varying (LPV) model of the car's mass (we know the mass as explained in the assumption part) and the current speed, illustrated through the following diagram:

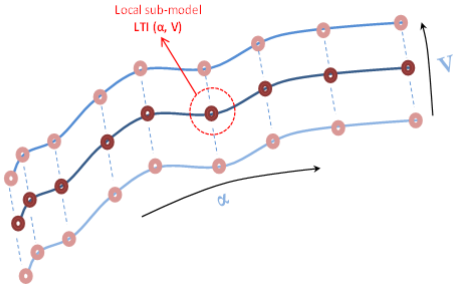

Figure 15: Illustration of grid-based gain-scheduling.

Source: https://www.mathworks.com/help/control/ug/plant-models-for-gain-scheduled-control.html

In principle, for each pair (mass, speed), we linearize the system, then form an interpolated array of linear state-space models. A certain number of points in the scheduling space are selected, forming a grid. An LTI system is assigned to each point, representing the dynamics in the local vicinity of that point. The dynamics at scheduling locations in between the grid points is obtained by interpolation of LTI systems at neighboring points. During the control process, interpolation would be used to schedule suitable gains for the system. This way we can make our controller adaptive and thus solve the problem of varying parameters. For now, we have implemented 25 different mass values (in kg) ranging from very light to very heavy load, and 11 values of reference speed (in m/s) to cover the whole range of speed according to an earlier study of Péter Gáspár (8)). We would change these ranges later when we come to the stage of combining the two parts of our project.

3.2.4 Gain-scheduled LQR with integral action and on-line road slope compensation

In this strategy, the control signal consists of:

$$u(t) = u_0 + \tilde{u}(t) = u_0 + \tilde{u}_{feedforward}(t) + \tilde{u}_{feedback}(t) \tag{34}$$

The feedback part is the same as the the gain-scheduling case. The feed-forward part is to compensate for the slope, which we know on-line (stated in the assumption part), and the rolling resistance:

$$\tilde{u}_{feedforward}(t) = mgC_r + mgsin(\theta(t)) \tag{35}$$

This way we can largely get rid of the effects caused by the slope. In our simulations, we model the noise when measuring the slopes by adding the small portion of the values to themselves.

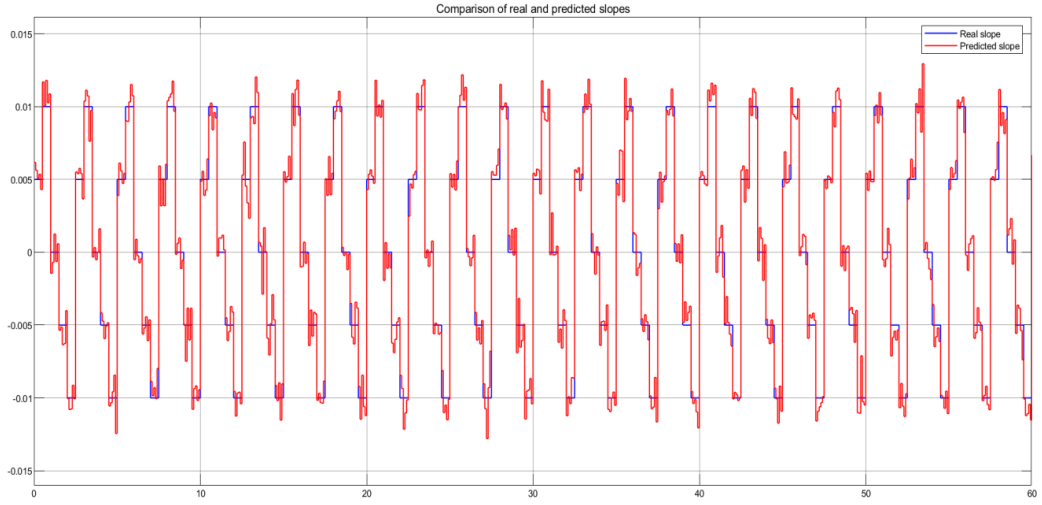

Figure 16: Real and compensating slopes

3.3 Validation of results

3.3.1 Analysis of uncertain parameters and disturbances

As stated above, the problem includes some uncertain parameters whose effects on the system we need to analyze and compare across controllers.

Methodology:

To analyze the effect of the system's uncertain parameters and disturbances, we would like to use the following model of implementing three controllers mentioned earlier under the same condition. For each of them, we calculate the root mean square error (RMSE) between the reference and the actual speed, first in the case every parameter remains at its own nominal value, and then each of them increases until it reaches 150% of its nominal value. The percentage change in RMSE with respect to the RMSE in nominal case:

$$\Delta RMSE = \frac{|RMSE - RMSE_{nomial}|}{RMSE_{nomial}} \tag{36}$$

Is then expressed in function of the change of the respective parameter in a graph from which we analyze that parameter. The smaller this change, the less sensitive the system is to the difference in parameters.

The car's mass:

This value depends on the passengers and the extra load in the car. When the car is made and the controller is designed, we know only the nominal mass. So we expect there would be changes in the mass when the car is used: either there are some passengers, or some luggage would be loaded onto the vehicle. We would want to analyze the effect of this uncertainty on the quality of control, by doing a simulation in which the real mass and the nominal mass are different. In the simulations before, the car's actual mass was 1410 kg, which corresponds to a Megane.

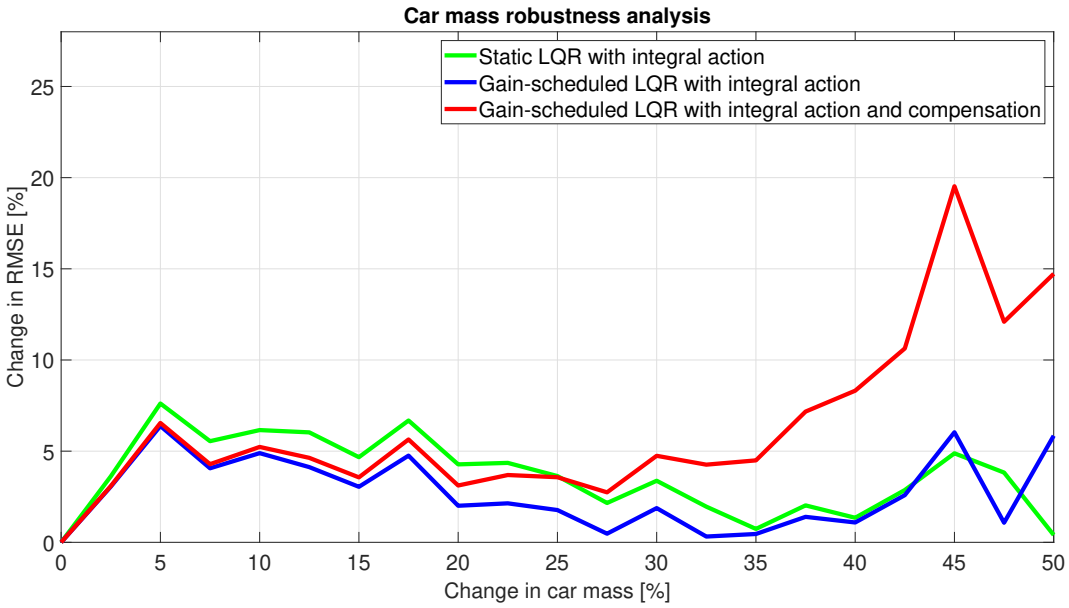

Figure 17: Analysis of the car mass uncertainty

We see that this uncertainty has a considerable effect on the quality of control (around 20% of change in RMSE). The case with scheduled gains was indeed more robust than the case without them (look at the blue and green lines), and the case with compensation is more sensitive to the change in mass as the mass appears in the compensation. When the mass becomes to large, then the control force must increase accordingly to vary the speed, and the 3rd case is when this force is the largest (we will see this more clearly in 3.3.2 when we simulate the systems in time domain). So it will saturate the force and make this controller work less effectively when we load too much weight onto the car. It is worth noting that the objective of this compensation startegy is not for greater robustness, but for a smoother response. So it is understandable if the compensation renders the system less robust, providing it is still more robust than the case with a static controller.

The road profile, represented by the magnitude of the slope:

This uncertainty as it affects the system through two forces: the road friction and the gravitational force. We would like to test the difference between the cases with and without compensation:

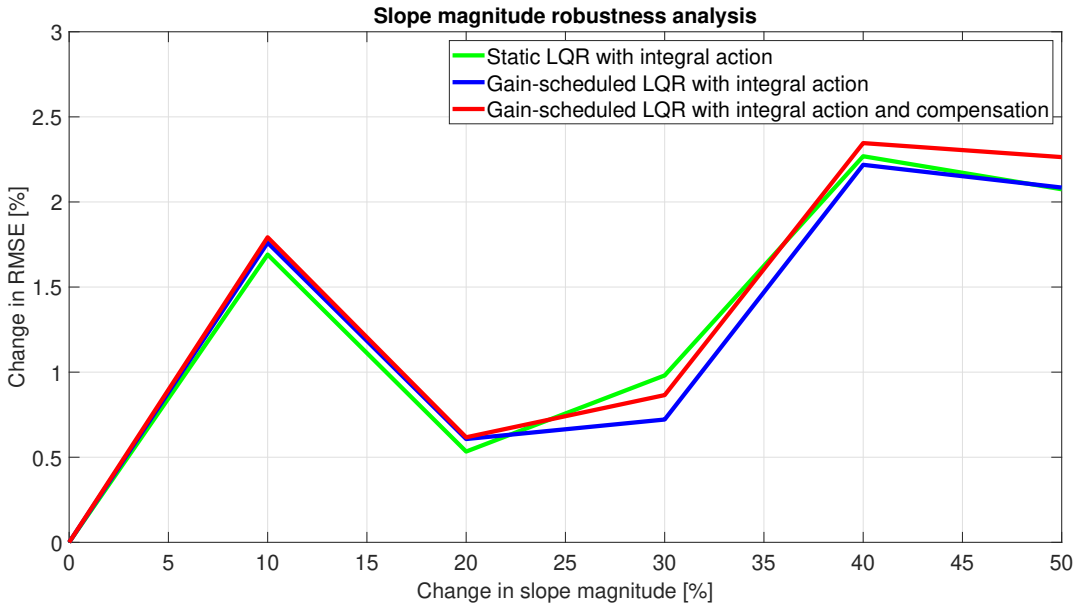

Figure 18: Analysis of the slope uncertainty

The first remark is the difference across the 3 controllers can hardly be seen and overall the RMSE changes very little (less than 2.5%) when the slope's magnitude increases by 50%. We see that even though the slope appears in 2 forces, its effect on the system is not quite significant. The case with slope compensation is indeed more sensitive to changes in slope magnitude, as we can see for the red and blue lines.

The rolling resistance coefficient C_r:

This uncertainty affects the system through road friction. This value depends greatly on the actual tire and road conditions, so at the time of building the controller, we can only implement a nominal of it. An analysis of this parameter's influence was performed in which we used different values for controller design and simulation:

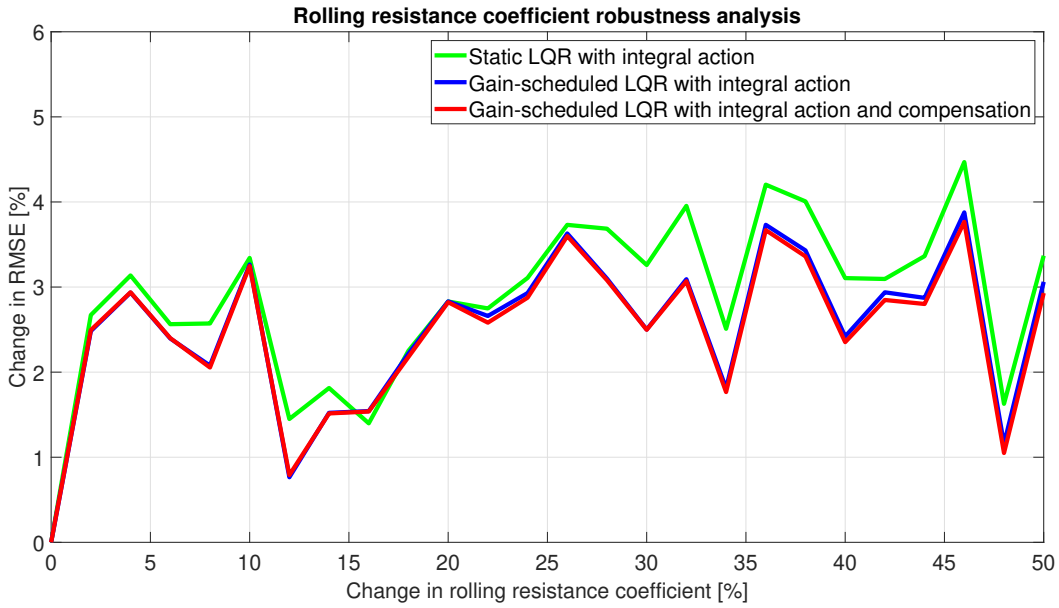

Figure 19: Analysis of the rolling resistance coefficient uncertainty

We have no significant difference, even though the 3^{rd} controller is the most robust one here, and scheduled gains work better than static gains. The influence of this uncertain parameter is negligible. We can safely use the nominal value of the road friction coefficient when designing the controller.

The actuator dynamics:

This value deals with how fast our actuator can response to the input signal which is the controller's force. According to a study (9), the actuator is modeled as a 1st-order system of unit static gain and a time constant of 0.1s which means a settling time of 0.3s.

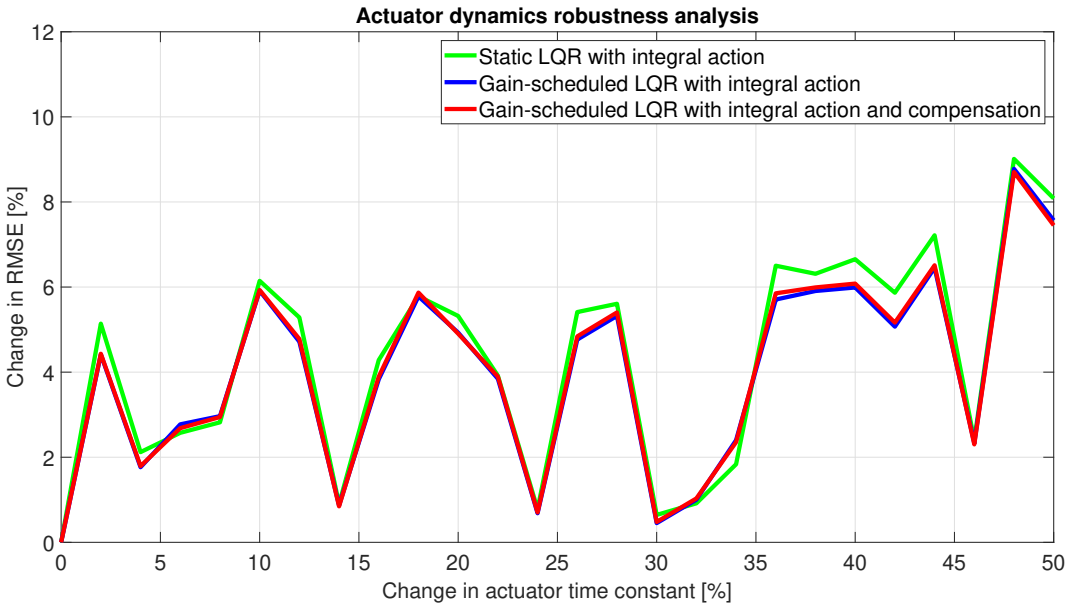

Figure 20: Analysis of the actuator dynamics uncertainty

This parameter results in insignificant changes in RMSE. We see that gain-scheduling is definitely more robust than static gains, and that there is almost no difference between the cases with and without compensation.

The communication delay:

According to the publication mentioned in the last part(9), the communication delay can take a nominal value of 0.2s.

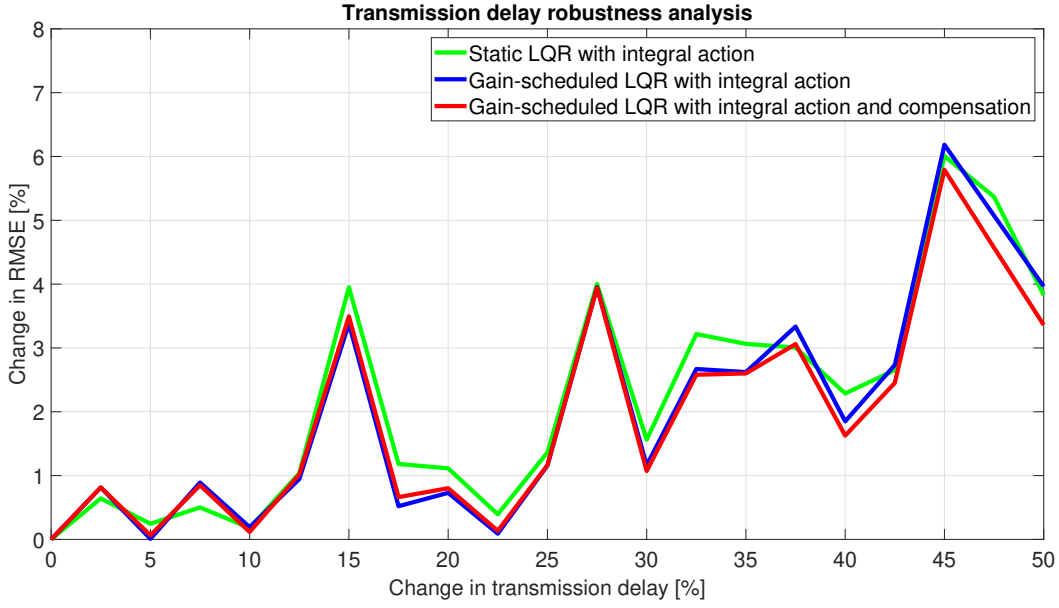

Figure 21: Analysis of the communication delay uncertainty

We notice that this time the static case is more robust when the change in the transmission delay is small, but less robust when the change becomes large. The case which compensation is the overall most robust.

The wind speed:

This value is completely random as it depends on nature. We would like to analyze its effect as a disturbance, which is why we always need integral action in the system's controller, regardless of its being a pole placement one or an LQR.

The average normal wind speed is from 12 to 18 km/h. Note that depending on the wind's direction, this force can speed up the car or slows it down. We added this when simulating the aerodynamic force:

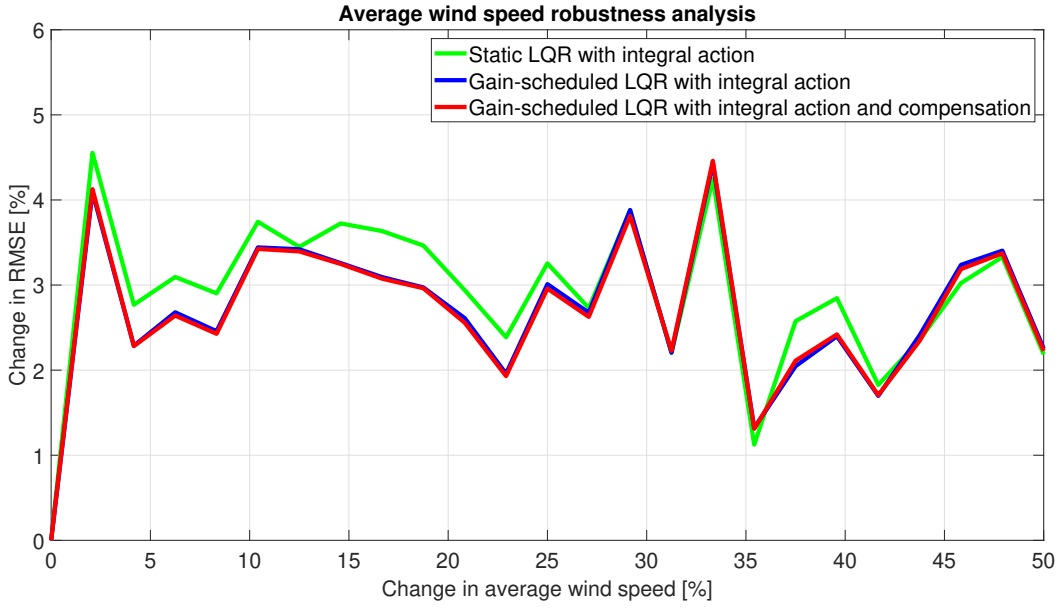

Figure 22: Analysis of the wind speed uncertainty

Some impacts were noted, but the integral action did a good job of rejecting this disturbance. The gain-scheduling and compensation still proved their superior robustness.

This is a summary of the controlled systems' robustness analysis:

Uncertain parameter	Influence	Corresponding strategy
Car's mass	Considerable	Gain-scheduled LQR
Road profile	Very small	Compensation
Rolling resistance coefficient	Very small	Use nominal value
Actuator dynamics	Small	Use nominal value
Communication delay	Small	Use nominal value
Wind speed	Very small	Integral action

After the analysis, we can see that the best controller in terms of robustness would be the gain-scheduled LQR with integral action and on-line road slope compensation.

3.3.2 Tests with various reference speeds and road profiles

In this part, we test the 3 controllers under the same condition in different speed profiles to analyze their performance in time domain.

Single step reference speed:

The first basic experiment is to see if the vehicle can respond well to a single step reference under disturbances. The step size does not need to be big. To avoid the abruptness in the reference speed, we smoothed it will a 2nd-order transfer function whose settling time is 1s.

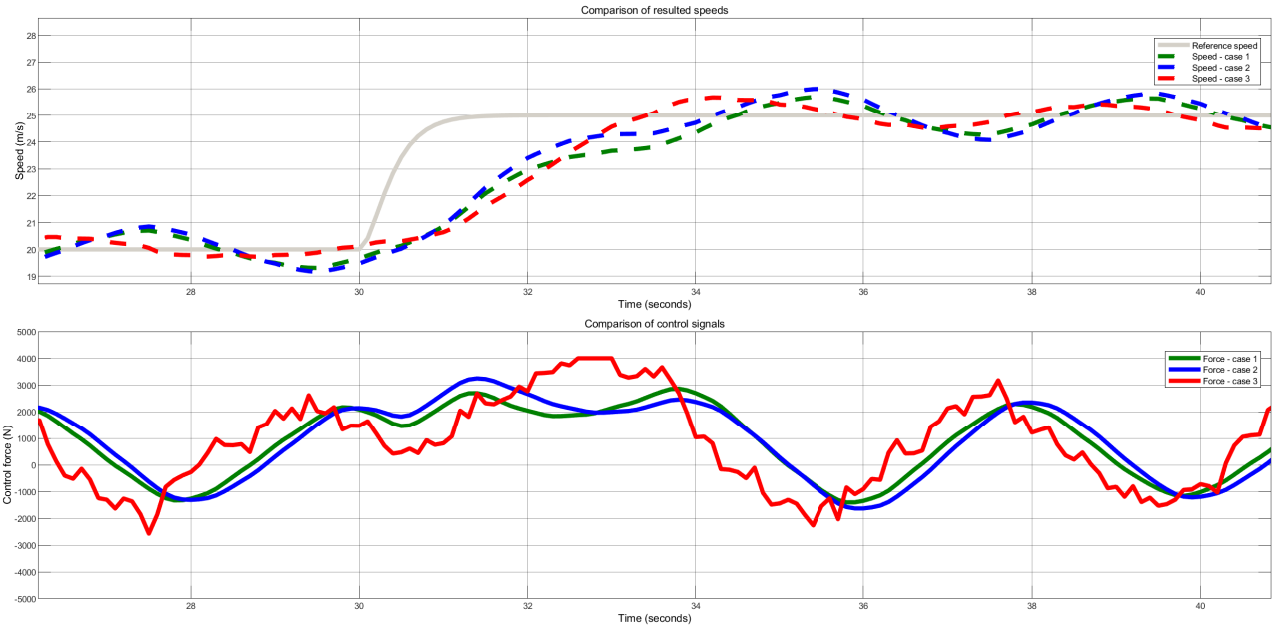

Figure 23: Test with a single step reference speed profile

We notice that the case with compensation is the fastest one to converge with a settling time of around 3s. Besides, its control signal varies in a complex manner (to compensate the slope) but never saturates. And it is true that for this controller, the control signal is the largest, which demonstrates our statement in the mass robustness analysis part. Its response is also the fastest one with the fewest fluctuations, which also helps to guarantee driving comfort.

Multiple step reference speed:

The second experiment is to see if the vehicle can perform a series of acceleration and deceleration under disturbances. This is the most common scenario in reality.

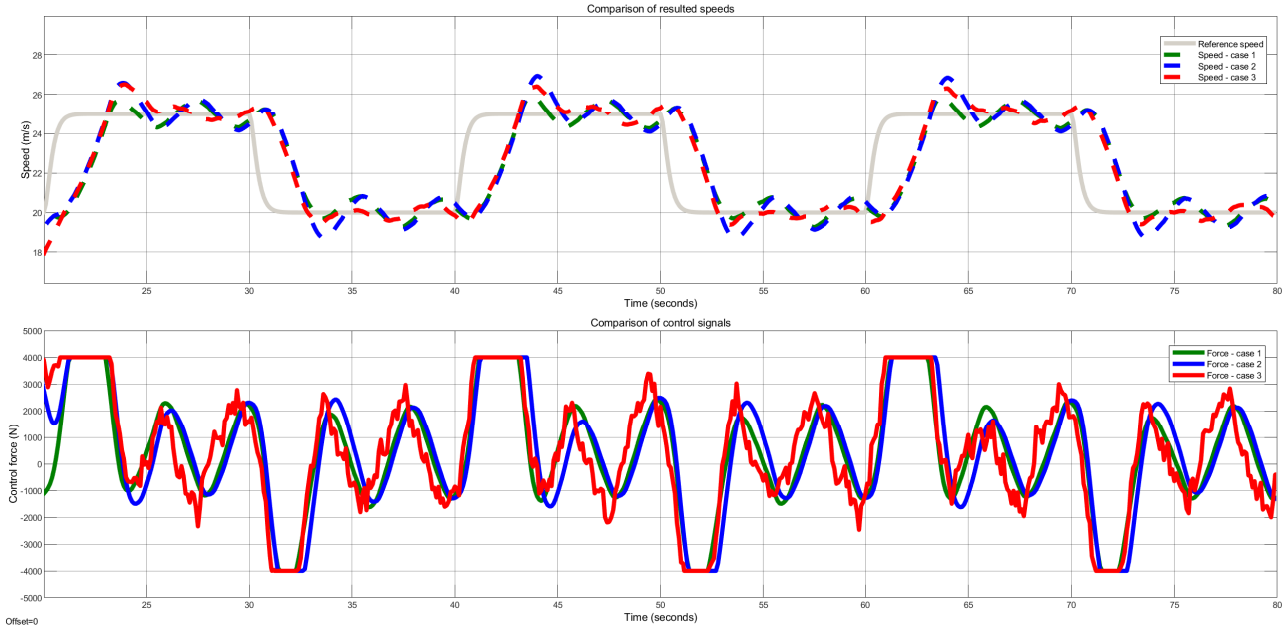

Figure 24: Test with a multiple step reference speed profile

This time we see that there are overshoots of around 20%, and for the gain-scheduling cases the overshoot is larger. However the 3rd controller smooths the response the fastest, compared to the other cases where the oscillation lasts even until the reference speed changes to its new value.

Large step reference speed:

The third experiment is to see if the vehicle can perform a sudden acceleration under disturbances, mainly to test the saturation cases.

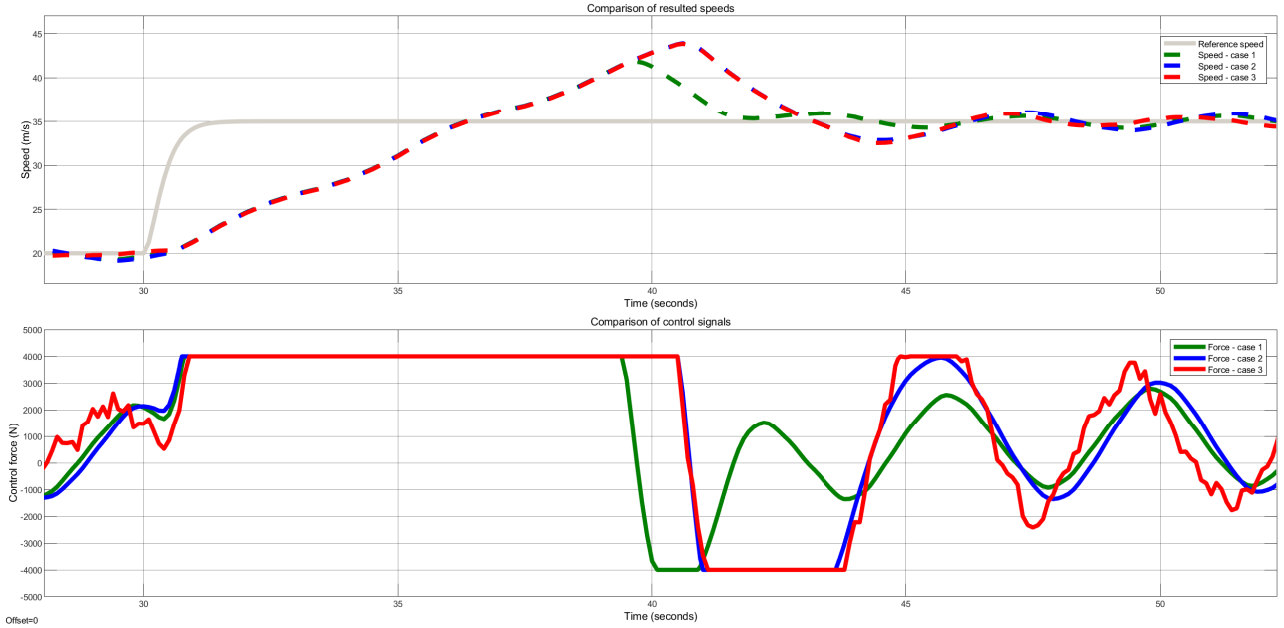

Figure 25: Test with a large step reference speed profile

This can also demonstrate the case of a sudden brake, where the reference changes to much that it saturates the engine. The control signal for the static case is the smallest so it results in the smallest overshoot, but still the difference is not significant. The case with compensation still gives the smallest oscillations.

Look-ahead reference speed with real road profile:

This speed profiles was from a study of Balázs Németh (8) in which they used a method called look-ahead to derive a reference speed. That was not based on comfort, however it is useful to test our controllers. We also have a real altitude profile from them which allows us to get a real slope profile by taking its derivative. These are the speed and slope profiles:

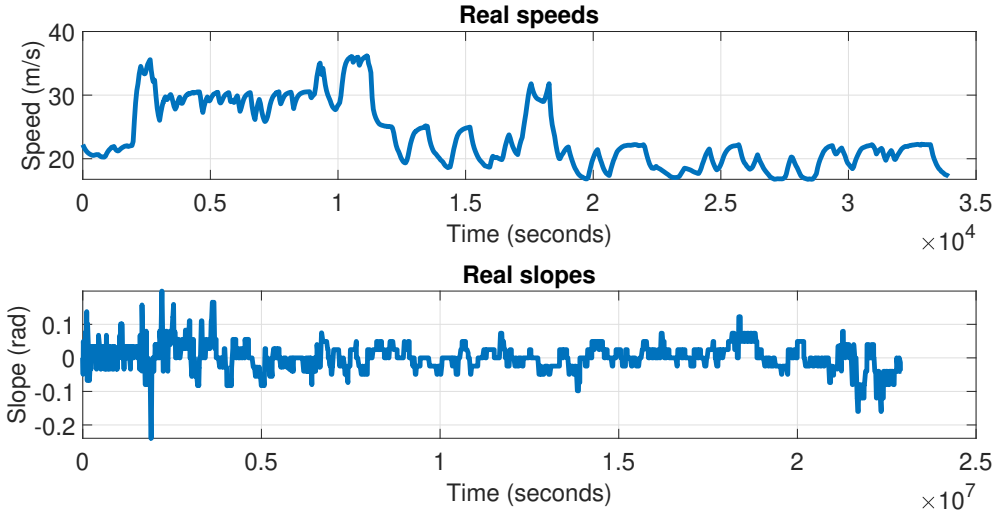

Figure 26: The real slope and reference speed profiles

Results of the test with the controllers:

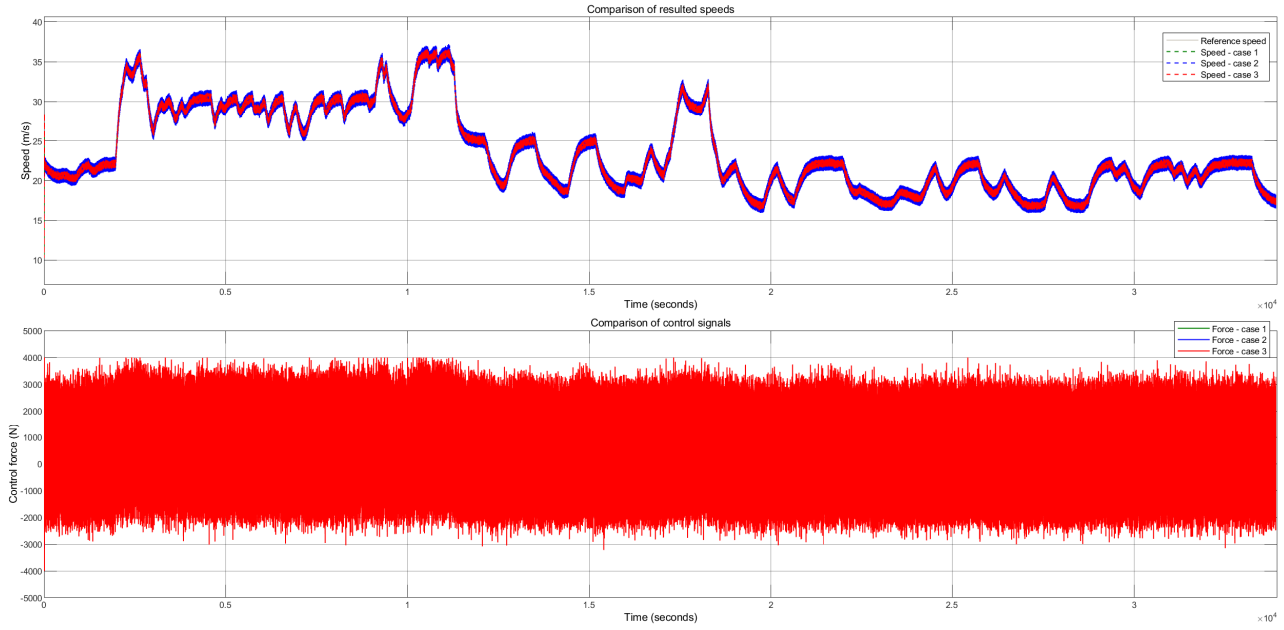

Figure 27: Test with a real reference speed profile

All the 3 controllers work fine in this realistic case. We hardly recognize the difference among them. After the uncertainty analysis and the tests with speed profiles, we conclude the control part by saying that the designed controller with gain-scheduling and compensation is good in terms of tracking, disturbance rejection, robustness and it passed well the speed profile tests by giving the smoothest response. It will be chosen for the combination part: comfort-oriented speed control.

4 Comfort-oriented speed control (This part has been mainly handled by Bao)

In this part we introduce the following structure used to model the car's longitudinal and vertical dynamics and control, as well as the comfort level. Then we will give the results of implementation of our work.

4.1 The structure

4.1.1 Objectives and necessary assumptions

The objectives of this combination part are to:

- Define a structure for the autonomous vehicle's computer that is effective in generating comfort-based reference speed values and control the car to track it under disturbances

- Evaluate driving comfort using the quarter car model and the RMS

The car's computer plays a crucial role in the model. This is a device programmed into the car which will use the information about:

- The road's slope and roughness: being a connected vehicle, our car has algorithms to detect these. This is the core part of comfort-oriented control, as we need to know the road type for all the calculations relating to comfort.

- The car's current speed: using the built-in speedometer

- The car's current mass: using built-in sensors that keep track of the additional load

- The values of the reference speed calculated with a comfort objective: stored in the memory

To control the vehicle's engine using a single control signal u. The wind force remains an unknown input disturbance of longitudinal dynamics. These assumptions are crucial for the design of such a computer.

4.1.2 The comfort-oriented longitudinal speed control structure

To generate correctly the control signal, the structure of the car's computer includes these components:

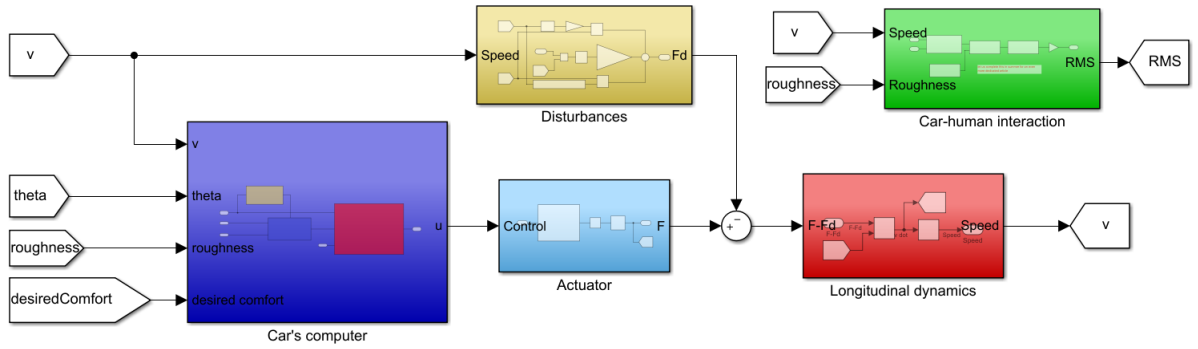

Figure 28: The proposed structure

The car's computer takes the mentioned input to generate a single control signal that would drive the engine. Inside this computer, we have three components:

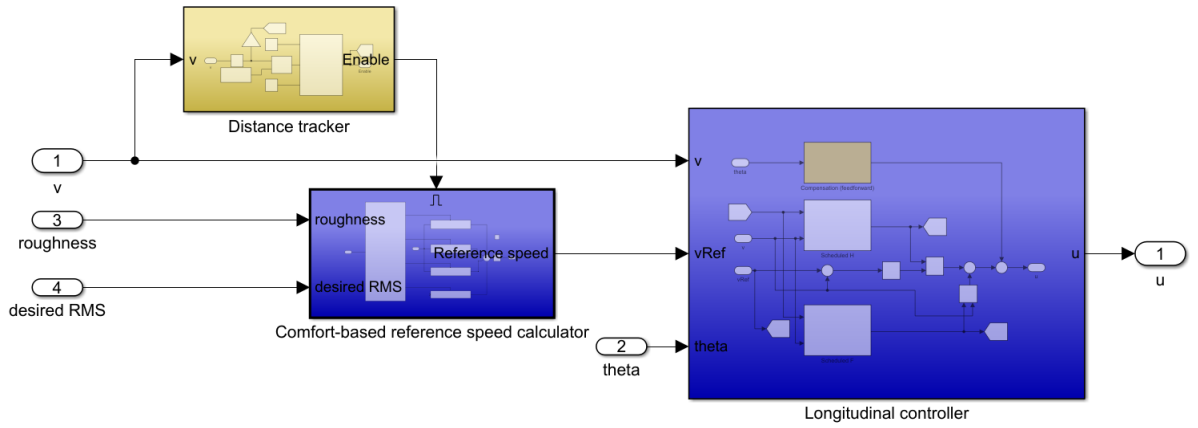

Figure 29: Components of the car's computer

The distance tracker keeps track of the distance traveled and enables the comfort-based reference speed calculator each time a certain distance has been reached (in our case it is 1 km). This calculator, thanks to the roughness that is known, schedules the reference speed according to the road type (here we have A-B, C, D and E) and the desired RMS level to generate the speed value and give this to the controller (gain-scheduled LQR with integral action and slope compensation). The controller then generates the control signal.

To model the car-human interaction, we use a quarter car model (we have 4 of these in a full car model). We assume that the 4 are identical given that the distance traveled is significantly larger than the car's size. The excitation (bump) from the road, $Z_r(t)$, is generated through the equation (3).

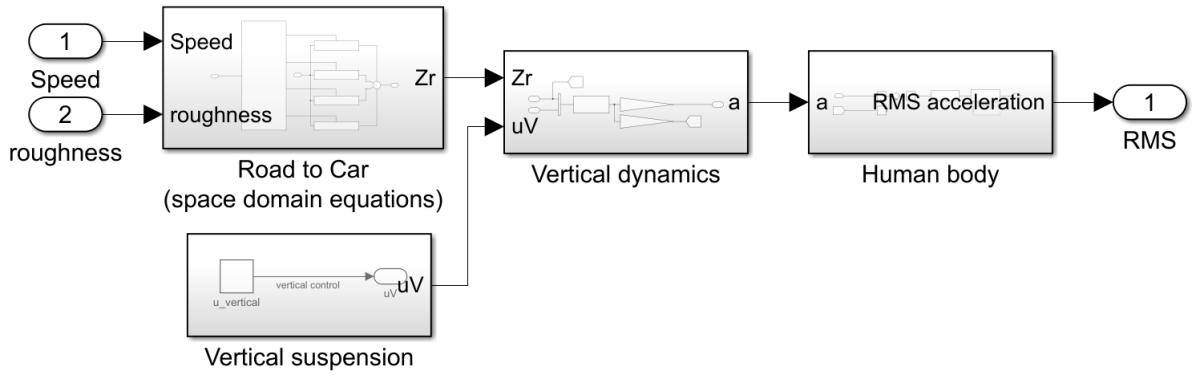

Figure 30: Modeling of the road and vertical dynamics

This excitation would be transmitted to the drivers and passengers through the quarter car model. As vertical control is not the focus of this study, we used a passive suspension system (vertical control = 0). To guarantee driving comfort, a semi-active suspension system is necessary here.

The acceleration transmitted to the humans would then go through the ISO 2631 filter which modelizes the human's vibration frequency range. We added an algorithm which calculates the RMS of the acceleration in a finite horizon T according to:

$$a_{RMS}(t) = \sqrt{\frac{1}{T}\int_{t-T}^{t} a_w^2(\tau)d\tau} \tag{37}$$

Which is used to evaluate comfort in time. Note that since T is defined at the time to travel 1 km, it is not a constant value.

4.2 Simulation results of comfort-oriented speed control

The algorithms we proposed worked effectively: each time a 1 km distance has been made, a new comfort-oriented reference speed is generated and the car automatically tracks this value. This is the core objective of our project. Here we simulated a drive on a road whose type varies from A-E in a random manner. Thanks to the estimation algorithms, the car detects the actual road type and adjusts its speed strategically.

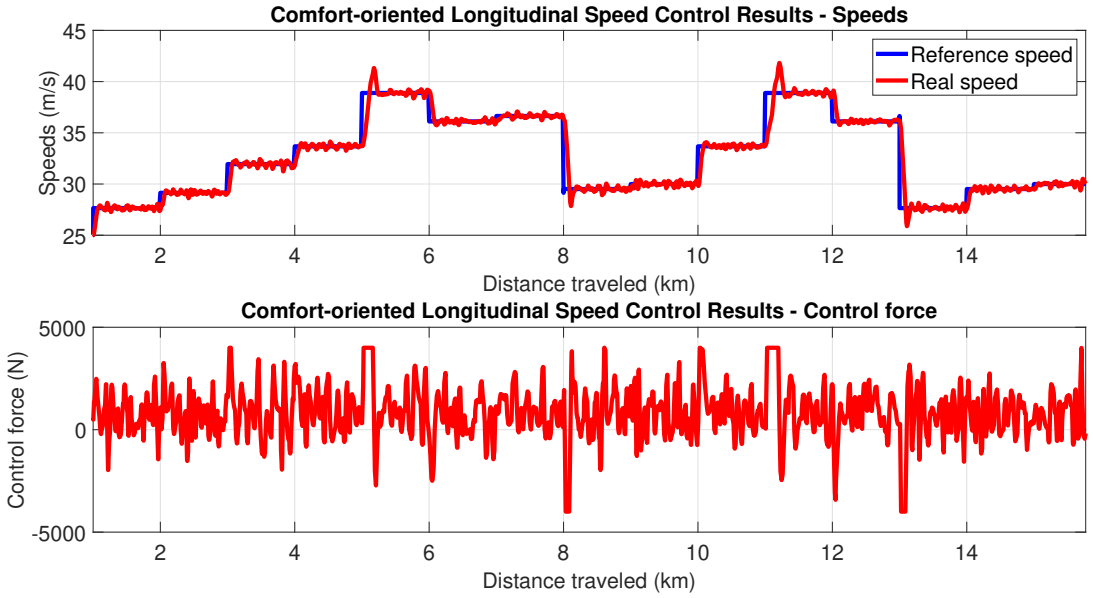

Figure 31: Results of comfort-oriented longitudinal speed control

We also evaluated online the RMS acceleration felt by the humans through a one-hour drive on a road of type A-B (not very bumpy), as the first steps of comfort evaluation and control. Here we have clearly a trade-off between speed and comfort. If we want to go fast then the driver risks getting large values of RMS and vice-versa. In our experiment, the level of RMS desired is updated after each 15 minutes and we watch how the actual RMS changes accordingly.

It is clear that the actual RMS rises and falls whenever we want it to rise and fall, but it could not track the "reference RMS". We explain this by stating that this is not a closed-loop controlled variable, but instead open-loop. If we want to "control" the comfort level we would have to feed it back like we are doing with the speed. Such an activity is almost redundant in this case as:

- The RMS depends greatly on the road type, which is considered as random (we can estimate it with our algorithms, but it varies quite randomly).

- The RMS is a value perceived by us humans which is not measurable like the speed with the speedometer. This is more like a "feeling" which we can only estimate.

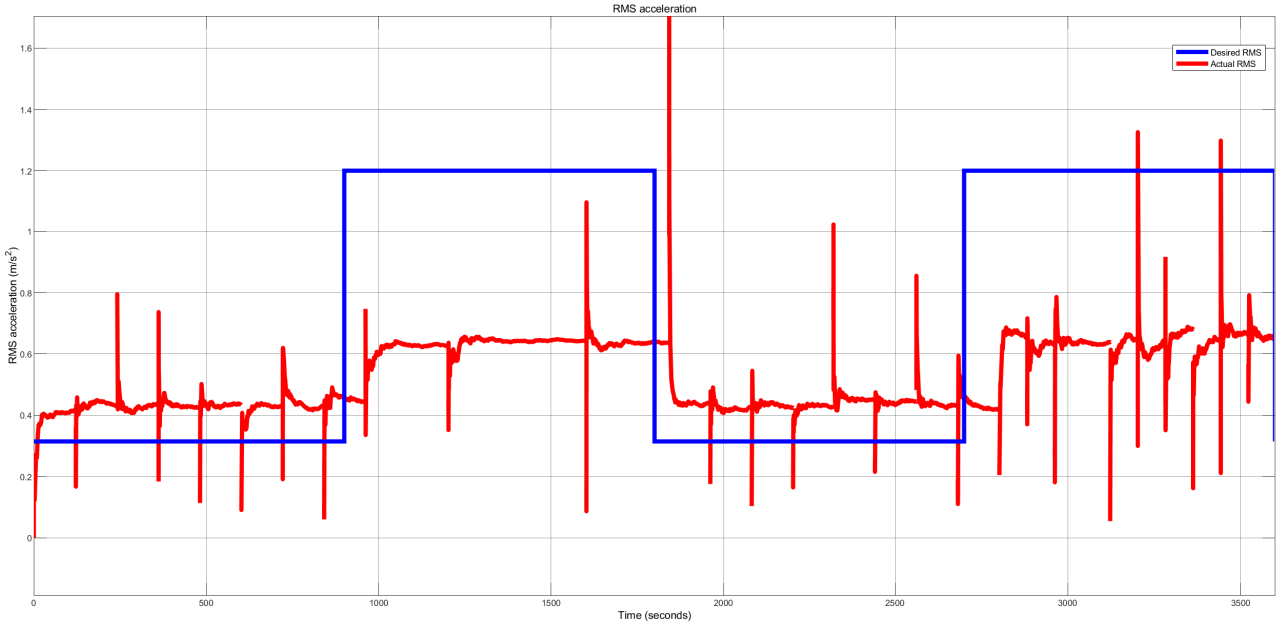

Figure 32: Comfort evaluation - the first steps

Note that this RMS value is calculated after each distance increment. The "discontinuities" are explained as the change when the RMS equation resets. The RMS then converges to its value for the horizon.

We then notice a trade-off: if we allows more discomfort, then the speed is allowed to raise accordingly. The car "understand" this automatically by raising the reference speed. We can see that the high speeds correspond to the high RMS values allowed.

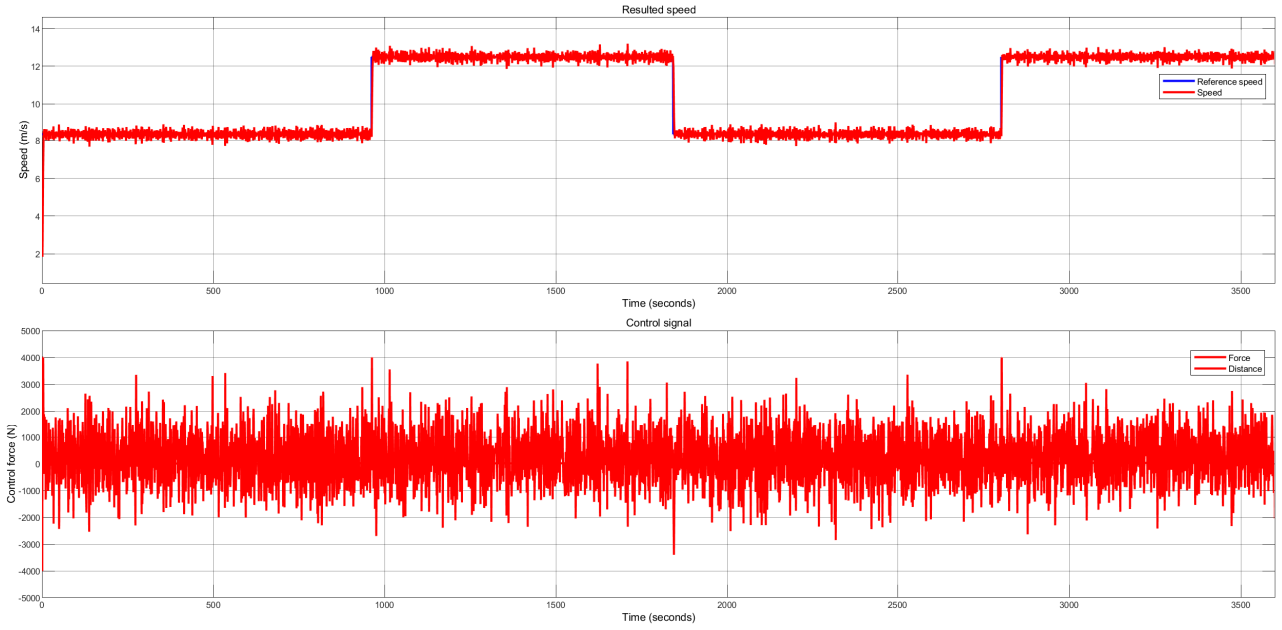

Figure 33: RMS-speed trade-off

As a result, the bump from the (same) road has its magnitude increased from 4 cm to almost 6 cm whenever the speed is raised.

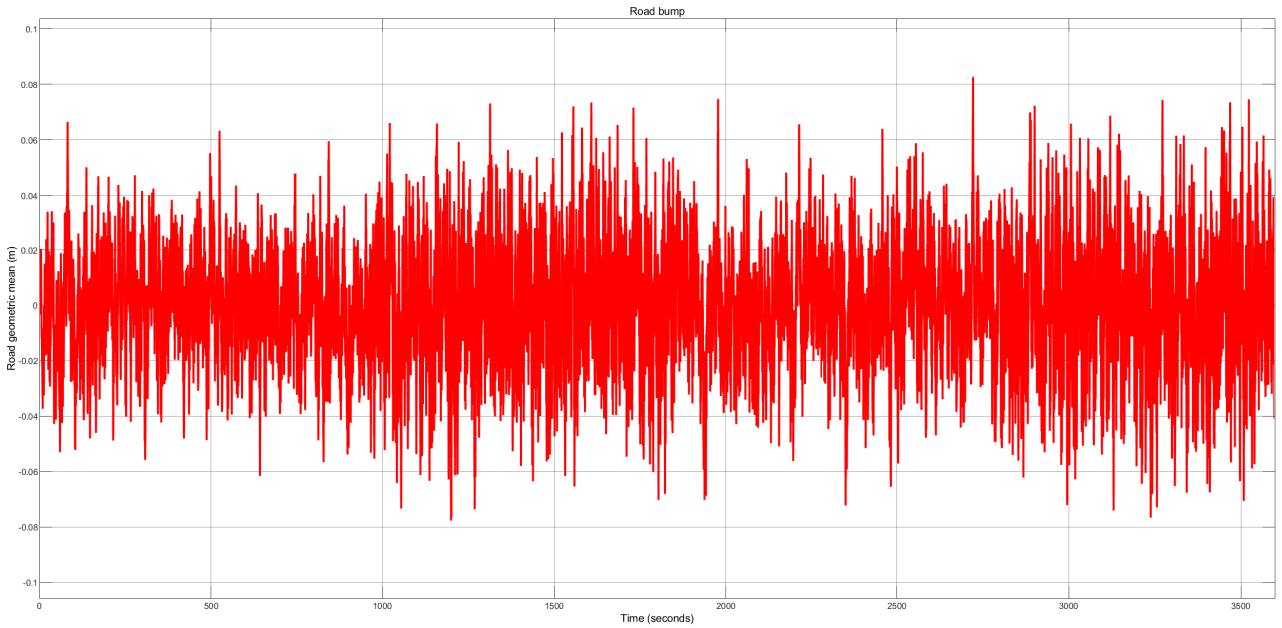

Figure 34: Road excitation

This bump is transmitted to the seat through the vertical dynamics. This result below confirms the speed-RMS trade-off. As the speed goes up, the oscillation transmitted to the driver increases, and so does the level discomfort.

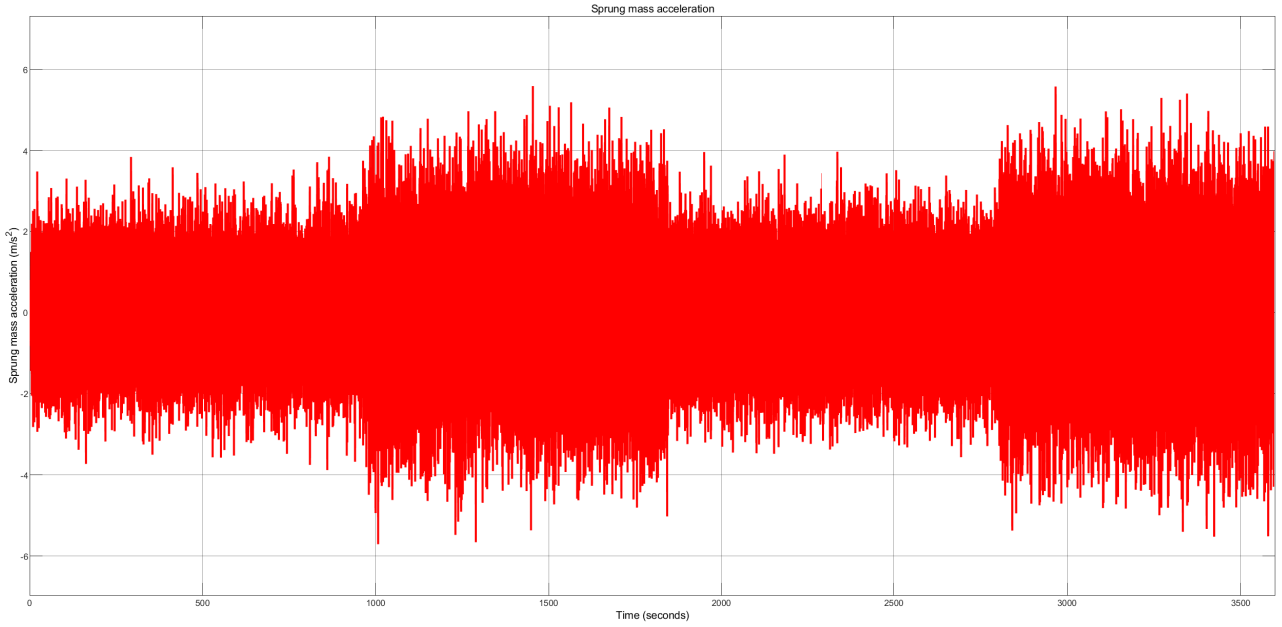

Figure 35: Acceleration of the sprung mass

5 Conclusion

5.1 Remarks about the project - results, problems, competencies developed

After building the road profiles and applying the ISO2631 filter, it was possible to start the analysis from a comfort point of view. And after tracing the comfort level for each type of road profile with different speeds, we were able to build a relationship between the speed, the comfort level and the road profile. This way we obtained a level of comfort for a certain road profile depending on the speed.

Then, we successfully built and tested different longitudinal speed control approaches for an autonomous vehicle. We also proposed and implemented a comfort-oriented speed control strategy which gave favorable results.

Competencies developed: system modeling (vehicle dynamics); simulation, analysis, and evaluation of results; finding and reading scientific documents; presenting project orally and in written form, English skills.

We proposed two articles to The 17th International Conference on Vehicle System Dynamics, Identification & Anomalies (VSDIA), Budapest, Hungary, November 2020:

1/ Eduarda Costa, Thanh Phong Pham, Olivier Sename, Gia Quoc Bao Tran, Trong Tu Do & Péter Gáspár, "Definition of a Reference Speed of an Autonomous Vehicle with a Comfort Objective"

2/ Gia Quoc Bao Tran, Olivier Sename, Péter Gáspár, Balázs Németh Eduarda Costa, "Adaptive Speed Control of an Autonomous Vehicle with a Comfort Objective"

In order to complete the big picture, we would need to:

- Collect experimental data when the laboratory reopens: generate the Zr(t) pulses and observe the RMS results.

- Add a semi-active suspension system: to really complete the big picture. We already have many studies on this so we can just apply a controller that we feel the most appropriate (test them like we did with our controllers).

5.2 Future developments

This project serves as a very first milestone in our journey with comfort-oriented vehicle control approaches. We propose some possible ways to develop this topic:

- Try the vertical control approach to further guarantee comfort.

- Try to control in closed-loop the RMS by feeding it back and designing some further algorithms to schedule the RMS. So we have both generators of the reference speed and the RMS before the controller, all in our car's computer.

- Build a mass observer of type LPV: by extending the system we can estimation of the car's mass using the system's input and output. We already tried several approaches for this idea during this project but they are not yet completed: normal observer, reduced-order observer, LPV observer, least-squares optimization algorithms. This would raise another trade-off problem between on-time scheduling and lower price.

6 References

References

[1] Y. Du, C. Liu and Y. Li, "Velocity Control Strategies to Improve Automated Vehicle Driving Comfort" in *IEEE Intelligent Transportation Systems Magazine*, vol. 10, no. 1, pp. 8-18, Spring 2018.

[2] Agostinacchio, M. & Ciampa, Donato & Olita, Saverio. (2013). The vibrations induced by surface irregularities in road pavements – a Matlab® approach. European Transport Research Review. 6. 267-275. 10.1007/s12544-013-0127-8.

[3] Prashant R. Pawar, Arun Tom Mathew, M.R. Saraf, IRI (International Roughness Index): An Indicator Of Vehicle Response, *Materials Today: Proceedings*, Volume 5, Issue 5, Part 2, 2018, Pages 11738-11750,

[4] Péter Gáspár, Zoltán Szabó, József Bokor, and Balázs Németh: "Robust Control Design for Active Driver Assistance Systems. A Linear-Parameter-Varying Approach", *Springer Verlag*, 2017.

[5] Gillespie, T. 'Everything You Always Wanted to Know about the IRI, But Were Afraid to Ask!' Road Profile Users Group Meeting September 22-24, *Lincoln, Nebraska*, 1992.

[6] Ahlin, Kjell & Granlund, Johan. (2001). Calculation of Reference Ride Quality, using ISO 2631 Vibration Evaluation

[7] Kjella Ahlin & N.O. Johan Granlund (2002) Relating Road Roughness andVehicle Speeds to Human Whole Body Vibration and Exposure Limits , International Journal of Pavement Engineering, 3:4, 207-216, DOI: 10.1080/10298430210001701

[8] Balázs Németh and Péter Gáspár (2011). LPV-based control design of vehicle platoon considering road inclinations. The International Federation of Automatic Control, *Milano*, *Italy*

[9] Oncu, S., Ploeg, J., Wouw, van de, N., & Nijmeijer, H. (2014). Cooperative adaptive cruise control : networkaware analysis of string stability. IEEE Transactions on Intelligent Transportation Systems, 15(4), 1527-1537. https://doi.org/10.1109/TITS.2014.2302816